

SEISMIC ASSESSMENT AND STRENGTHENING OF THE REMAINING BEIRUT PORT SILOS DAMAGED AFTER THE 2020 AUGUST BLAST- A CASE STUDY

S. Ismail¹, W. Raphael² and F. Kaddah³

¹ Saint Joseph University of Beirut, Beirut 17-5208, Lebanon
sahar.ismail@net.usj.edu.lb

² Saint Joseph University of Beirut, Beirut 17-5208, Lebanon
wassim.rafael@usj.edu.lb

³ Saint Joseph University of Beirut, Beirut 17-5208, Lebanon
fouad.kaddah@usj.edu.lb

Abstract

In 2020, the Beirut port silos, located few meters away from the center of August 4 explosion, were severely damaged. The first and second row of Beirut silos/East side were destroyed. However, the third row of silos was damaged and experienced an immediate tilt, except the last two silos in the South block (silos #130 and 137) that were destroyed. As a result, the remaining standing silos, have been monitored since the day of the blast using 3D scan measurements and triaxial inclinometers, experienced severe tilting over time. In July 2022, the rate of silos' inclination increased after a fire broke out in the North block silos due to grains' fermentation. As a result, in August 2022, the last silos of the North block fell after resisting severe tilting for two years with a maximum permanent vertical inclination of 2 m. Consequently, the 8.5 m diameter-42 silos supported by a 2500 pile foundation consisted as of August 2022 of 6 standing South block silos. In this paper, the authors describe the status of these silos and the performed structural health monitoring. A 3D finite element model was built in Abaqus to analyze the behavior of the silos under different seismic loadings. The results are evaluated in terms of horizontal displacements at top of the silos which are used to assess the stability of the structure. The obtained results show that the South block silos will exhibit serious damage and possible failure in case of moderate intensity earthquakes. Therefore, a repair and strengthening method to preserve the remaining standing silos using numerical analysis is proposed.

Keywords: Damage, Collapse, Strengthening method, Blast Loading, Seismic Loading, Numerical Analyses.

1 INTRODUCTION

Civil structures deterioration with time is associated with environmental factors such as steel corrosion and concrete carbonation, aging in construction materials and extreme events such as earthquakes, hurricanes, floods, and blast loadings. As such, after these extreme events, Structural Health Monitoring (SHM) is used to provide quantitative and reliable data on the real condition of a structure. SHM is a damage identification technique for damage assessment and performance evaluation for aerospace, civil and mechanical infrastructures. It refers to the observation and analysis of the structure's damage and deterioration level over time using periodically spaced sensing measurements. Moreover, it is associated with life-safety and economic benefits [1 to 3]. Several non-destructive methods are used in SHM such as the wireless sensor networks to sense and collect data [4 to 6]. Recently, SHM has gained important interest in examining the status of health and maintenance of structures such as large-scale bridges [7 and 8].

On the 4th of August 2020, one of the most powerful non-nuclear explosions in history occurred in the port of Beirut, Lebanon [9]. This explosion ripped the city to shreds, caused more than \$15 billion in damage, and left more than 200 casualties and 7400 injuries. The August 4, 2020 explosion, was attributed to the detonation of around 1100 to 2750 tons of Ammonium Nitrate [10 to 18, etc.]. It created a crater of 90 m wide X 100 m long X 6 m deep and damaged several significant structures in the area, including the Beirut port silos. As shown in Figure 1, following the explosion, the first and second row of Beirut silos/East side were destroyed. However, the third row of silos was damaged and experienced an immediate tilt, except the last two silos in the South block (silos #130 and 137) that were destroyed (Figure 1 and 2). To assess and monitor the level of damage of Beirut port silos, the structural health monitoring SHM of Beirut port silos following August 4, 2020 explosion was performed by the school of engineering ESIB at Saint Joseph University of Beirut, Lebanon and Amann Engineering using 3D laser scan measurements and four ultraprecise triaxial inclinometers installed in strategic locations on the remaining standing silos (Figure 1 and 2).

The explosion generated an immediate 20 to 30 cm horizontal tilt in the silos, measured East to West. Since that time, the remaining standing silos have been tilting. In fact, the South block silos have been stabled since November 2020 while the North block silos tilt shifted since the blast West to East, towards the explosion crater. In July 2022, fire in the silos, caused by the fermentations of the remaining trapped grains in the silos that could not be removed for several reasons, caused an increase in the rate of silos' inclinations. As a result, silos # 35, 42, 33 and 40 fell on July 31, 2022, silos 49, 56, 47 and 54 fell on August 4, 2022, and silos # 63, 70, 77, 84, 82, 75, 68 and 61 fell on August 23, 2022 (Figures 1 and 2). Note that no injuries were reported following the collapses as the authorities' evacuated parts of the port area in anticipation of them.

Researchers have been studying the failure of real case studies structures including collapsed silos [19 to 23] to prevent future incidents. Since Lebanon is in an active seismic zone and its prone to several seismic events, the behavior of the remaining standing South block silos was simulated in this paper using the Finite Element Software Abaqus following different seismic loadings. The obtained data will serve as guidance of how a damaged structure can behave after a large explosion and partial collapse. Finally, following the decision of the Lebanese authorities to preserve the remaining tilted standing silos to serve as a memorial for August 4, 2020 explosion, a repair and strengthening method of the South block silos using numerical analysis is presented.



Figure 1: a) The damaged grained Beirut port silos, after August 4, 2020 blast [24] and b) The collapse of the North block silos [25].

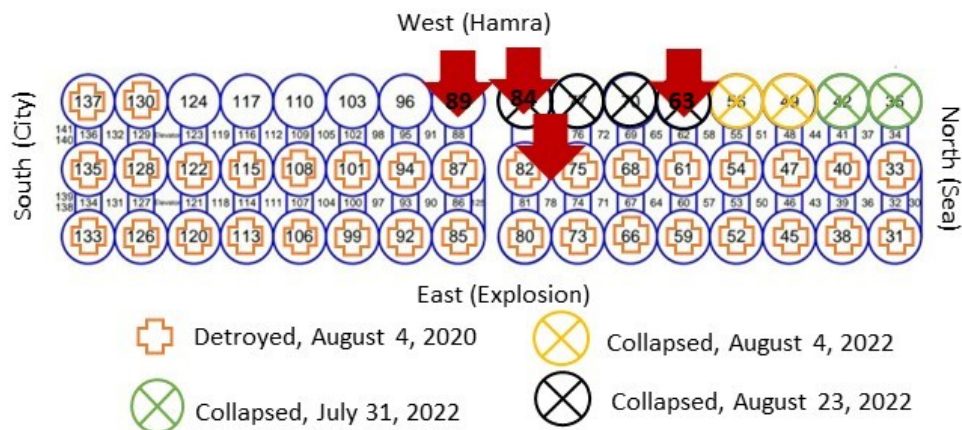


Figure 2: Silos' name tag, status, and tiltmeters' positions Beirut port silos.

2 BEIRUT PORT SILOS

The grain storage Beirut port silos were built in 1968 in three phases at a cost of \$2.8 million. Beirut port silos, the largest grain facility at the time, was equipped with loading and unloading equipment for ships, railway wagons and cars [26]. As shown in Figure 3, engineers constructed 24 silos formed of 8 columns X 3 rows during phase 1 (in 1968), 18 silos formed of 6 columns X 3 rows during phase 2 (in 1969) and 6 silos formed of 2 columns X 3 rows during phase 3 (in 1997). Thus, the silos, completed and put into operation in 1969, consisted of 14 columns X 3 rows of 48 m high, 8.5 m diameter cylindrical silos with a bearing storage capacity of 105 000 tons of grains. And then in 1997, after the addition of 6 silos, the structures' grain storage capacity was increased by 15 000 tons of grains. Note that from 2000 to 2002, the engineers reinforced the inner walls of the outer silos due to concrete carbonation caused by the deterioration of the cells by the exposure to humidity and seafront. The inner wall of these silos was increased by 12 cm; the silos' original wall thickness was equal to 17 cm.

The concrete silos, constructed with a special water-resistant prescribed type of cement having a mean compressive strength of 30 MPa, were heavily reinforced. On average, the horizontal and vertical reinforcement are formed of 14-mm reinforced steel diameter every 180 cm and 12-mm reinforced steel diameter every 300 cm, respectively. As for the foundation, the Beirut port silos were built on 2500 square (30 X 30 cm) concrete piles driven to embedded lengths between 15 and 17 m in backfill soil consisting of 2 m of miscellaneous backfill

sand material and 15 m of sandy material that presents some levels of gravel and clay. Note that the water table was below the bedrock level.

The grain storage silos situated few meters from the center of the explosion, at about 70 m in front of the silos and 40 m from the side of the silos; based on the data of the Lebanese Army and Forensic Architecture, 2020, in warehouse 12 at the port, absorbed part of the blast energy and shielded some of the Western part of Beirut's structures. The August 4, 2020 explosion destroyed the first and second row of Beirut port silos (the East-face cylinders) while it damaged the third row (the Western-face cylinders) that has been tilting since the timing of the blast (Figures 1 and 2).

Following the explosion, the silos tilted 20 to 30 cm East to West with the highest deformation noted on silos #56 and 63 on the North block [11 to 15]. Even though the silos tilted away from the explosion crater at first (Hamra side), their rotation was shifted as of phase 1: West to East, towards the explosion crater. Note that, the collapse of the North block silos in August 2022, shredded by the massive August 4, 2020 explosion, was inevitable since the structure was beyond repair; severely damaged and unstable.

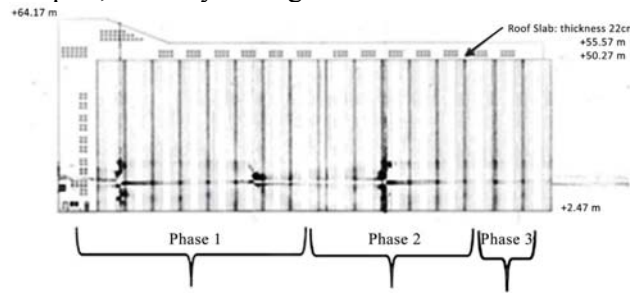


Figure 3: Vertical section and the construction phases of the Beirut port silos.

3 FINITE ELEMENT MODEL

The FE software, Abaqus, was applied to analyze the seismic behavior of the remaining standing Beirut port silos using three-dimensional model. The geometric model consisted of the 6, 8.5 m diameter, 48 m height tilted South block silos having a 29 cm wall thickness. The reinforced concrete silos were simulated using 4- node doubly curved shell, reduced integration, hourglass control, finite membrane strains S4R shell elements. Moreover, the silos steel reinforcement was defined as layers of reinforcement as part of the silos' shell elements using the rebars command (rebars' layers option) available in Abaqus.

The nonlinear behavior of the reinforced concrete under the static (the tilting phase) and dynamic loadings were modeled in Abaqus using the concrete damage plasticity model while incorporating strain rate effects (Figure 4). Moreover, the inelastic/plastic behavior of the steel reinforcement was simulated using elastic-perfectly plastic material by defining the steel yield stress. The relevant properties of the reinforced concrete and steel used in the FE model are presented in Table 1 and Figure 4. ρ = density (kg/m^3), E = Young modulus (GPa), ν = Poisson's ratio, σ_y = yield stress (MPa), K = the ratio of the second stress invariant on the tensile meridian, $fb0/fc0$ = the ratio of initial equibiaxial compressive yield stress to initial uniaxial compressive yield stress, ψ = dilation angle ($^\circ$), f'_c = concrete compressive strength (MPa). Note that the concrete and steel reinforcements in the silos were tied using the tie command in Abaqus and the base of the silos was assumed fixed.

The analysis in Abaqus contained two steps. First, the silos were displaced, based on the 3D scan and tiltmeters' data, to simulate their real movement since the day of the blast. Second, different seismic loads were applied at the base of the tilted silos, as detailed in Figure-

The seismic events were chosen having PGA values between 0.25 and 0.35g based on the seismic hazard for Lebanon study by [27] that shows that Lebanon is in zone 3 having a PGA value of approximately 0.25 g for a 475-year return period and 0.35g for a 950-year return period. Consequently, the structural status of the silos was generated. Note that a 5% damping ratio was considered in the analysis. Unlike the blast loading that resulted from August 4, 2020 explosion and released rapid hot gases, enormous amount of energy as well as high temperature and pressures in only milliseconds and produced a spherical-type wave that went from the superstructure to the foundation; the seismic loading forces the seismic wave to go up from the foundation to the superstructure and affects the system natural frequencies.

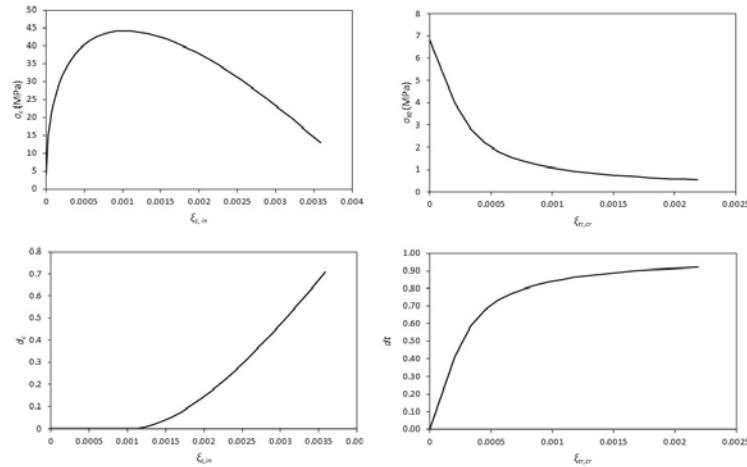


Figure 4: Stress-strain relation of the reinforced concrete in compressive and tensile region-concrete damage plasticity model with high strain rate effect.

Concrete	ρ (kg/m ³)	2400	Steel	ρ (kg/m ³)	7850
	E (GPa)	43		E (GPa)	206
	ν	0.2		ν	0.3
	ψ (°)	31		σ_y (MPa)	448
	Eccentricity	0.1			
	$fb0/fc0$	1.16			
	K	0.67			
	Viscosity parameter	0			
Backfill material	ρ (kg/m ³)	1500	Sandy Soil with some levels of gravel and clay	ρ (kg/m ³)	1700
	E (GPa)	40		E (GPa)	25
	ν	0.25		ν	0.25
	c (kPa)	2		c (kPa)	10
	Φ (°)	44		Φ (°)	38
	ψ (°)	2.5		ψ (°)	10

Table 1: Material properties

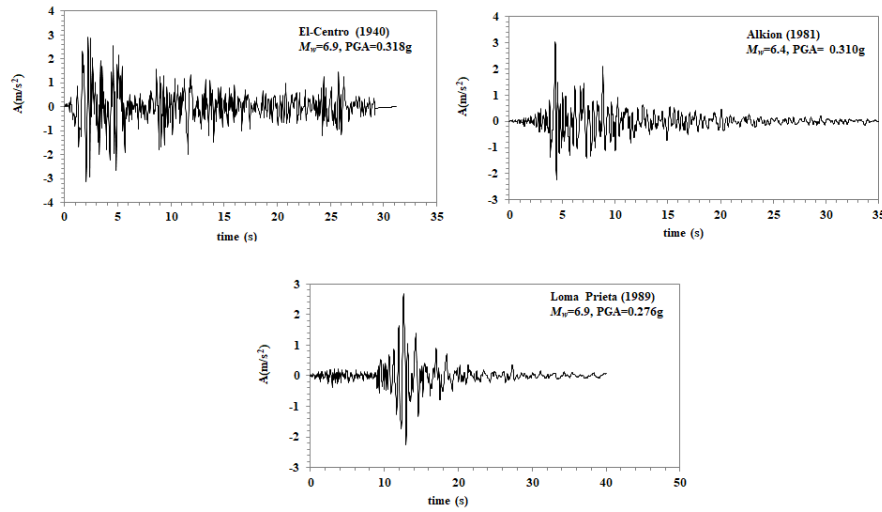


Figure 5: Acceleration with respect to time of El-Centro (1940), Alkion (1981) and Loma Prieta (1989) earthquakes.

4 RESULTS AND ANALYSIS

To study the effect of seismic loading, the displacement response of the remaining standing South block silos (Silos #124, 117, 110, 103, 96 and 89, as indicated in Figure 2) was investigated under 3 earthquakes: El-Centro (1940), Alkion (1981) and Loma Prieta (1989). The results, presented in Figure 6, indicate that the simulated seismic cases cause an immediate tilting of the silos towards the Hamra side (away from the explosion crater) under El-Centro (1940) earthquake and towards the explosion crater under Loma Prieta (1989) and Alkion (1981) earthquakes. In fact, the horizontal displacements of the stable South block silos increase from 3 to 30 cm (static condition, in February 2023) up to 73 cm under El-Centro (1940), while they decrease up to -1 cm under Loma Prieta (1989) and Alkion (1981), respectively (Positive displacement is towards the West/Hamra side while Negative displacement is towards the explosion crater). For example, the horizontal displacements at top of silos # 124 and 89 increase from 3 and 20 cm in February 2023 to 59.1 and 69 cm under El-Centro (1940) earthquake, while they decrease to 2 and 13 cm and -0.4 and 7 cm under Loma Prieta (1989) and Alkion (1981) earthquakes, respectively.

To present the state of damage of the simulated cases, the silos' damages in compression and tension were extracted from Abaqus. Figure 7 presents the South block silos' displacement, as well their status in damage and compression when hit by El-Centro (1940) earthquake. The amount of silos' damage, extracted from the FE model, presents the degradation of the silos' elastic stiffness, and is described by the compressive damage variable " d_c " (damage in compression) and the tensile damage variable " d_t " (damage in tension), where these damage variables range from 0: no damage to 1: destruction. Moreover, to show the state of damage of the silos' elements, the cumulative surface damage rate curves are plotted in Figure 8. The percentage of the damaged surface having undergone the amount of damage indicated is presented on the ordinate and the damage indicator (1 refers to completely damaged elements/surfaces) is presented on the abscissa. As shown in Figures 7 and 8, only 30% of the silos' surface underwent some level of damage. As detailed in Figure 8, only 27% of silos surfaces were 100% damaged under Alkion (1981) while only 18% and 13% of silos surfaces were 100% damaged under El-Centro (1940) and Loma Prieta (1989). The obtained results are in accordance with the North block silos' mode of failure depicted after their collapse. The

tilted silos fell on themselves without marking severe damaged surface first. As a result, any seismic load experienced in Lebanon will cause an important tilting of the remaining standing silos ending in severe silos' displacement, damage and high-risk of collapse.

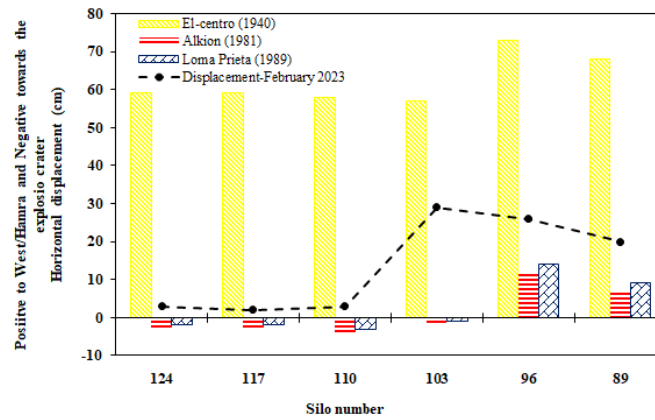


Figure 6: Maximum horizontal displacements at top of the South silos under different seismic loadings.

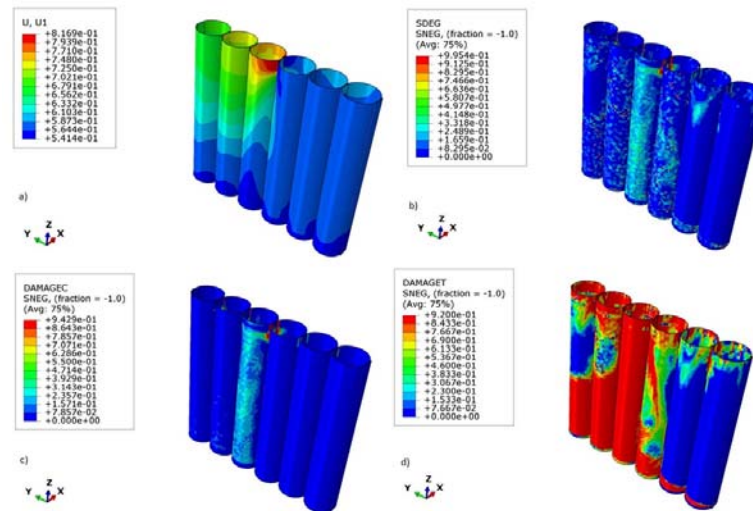


Figure 7: a) Horizontal displacement, b) SDEG output b) Damage in Compression and d) Damage in Tension (Damage variables range from 0 (no damage) to 1 (destruction)) of South Block silos hit by El-Centro (1940) earthquake (fixed-based case).

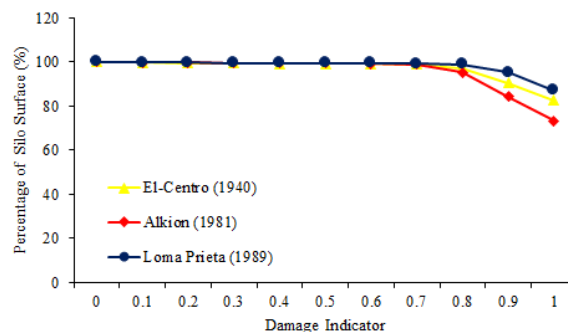


Figure 8: The cumulative surface damage rate curves of the different simulated cases.

5 REPAIR AND STRENGTHENING METHOD

As depicted by the 3D scans and tiltmeters' data obtained by [11-15], the high rate of the silos' tilting over the past two and half years was manifested by the appearance of new cracks on the bottom of the silos' walls. These cracks values mean that the damage is not superficial but deep and extends to the pile foundation. In fact, Ismail et al. [12-14] obtained that the pile cap as well as the head of the driven piles displaced on average 35 cm in the direction of the explosion. This value exceeds the allowable limits in all design codes, indicating that the piles' head deformed beyond their elastic limit and thus, the piles are severely damaged.

An explosion on the ground surface produces an air blast pressure as well as a ground shock near the structures that lie close to the detonation point, such as in the case of Beirut port silos. As mentioned previously, Beirut port silos in the late 1960s were built in 2 phases on predominantly sandy fill soil with a silty nature. The percentage of fines varies in the soil beneath the silos. Nevertheless, the highest percentage is located below silos # 126, 128, 130, 133, 135 and 137; i.e. below the destroyed South block silos. The blast exposed but did not widen the 1.2 m concrete gap at the construction joint between the Phase I and Phase II silos [11-15]. Moreover, the office building located next to the South block was destructed by the blast in addition to the first two silos of the South block: silos #137 and 130. Since the 30 X 30 cm, 15 to 17 m length slender piles were not designed to resist a lateral stress such as the one created by the underground component from the blast, then the closer to the explosion epicenter, the more likely the piles got damaged. As observed by the 3D scans and tiltmeters' data [11-15], the rate of silos' inclination increased during the wet season. As a result, the observed cracks at the bottom of the silos caused by the movement of the silos, indicate that the underground concrete piles are heavily damaged, and the structure-foundation-soil platform is getting compacted and sinking into the ground. In other words, the remaining standing silos are rested on damaged pile foundation.

Following the decision of the Lebanese authorities to preserve the remaining tilted standing silos to serve as a memorial for August 4, 2020 explosion, we present hereafter using Abaqus, a repair and strengthening method of the remaining standing South block silos. As such, the strengthen three-dimensional model was formed of the tilted reinforced concrete silos, the pile cap, the pile foundation, and the soil medium. The silos' wall thickness was increased from 29 to 41 cm. Moreover, the pile cap size beneath the remaining South block silos was increased by 3 X 1.12 m from the sides (length X thickness). Finally, 30 X 30 cm, 15 m length square driven piles were inserted below the new pile cap every 1 m. The pile cap and piles were embedded in a 200 X 200 X 17 m soil medium. The first 2 m of the soil profile were defined as miscellaneous backfill sand material while the next 15 m were defined as sandy material that presents some levels of gravel and clay. To account for the absorbed energy from the unbounded soil domain, the far-field soil, in both horizontal directions, was modelled using 8-node linear one-way infinite brick elements CIN3D8 [28]. Finally, to simulate bedrock conditions, the bottom soil boundary was defined as a rigid boundary. Table 1 details the material properties adopted in the numerical model. In Table 1, c is the soil cohesion (kPa) and Φ and ψ are the friction and dilation angles ($^{\circ}$). In this study, the silos, pile cap, piles, and soil were modelled by tying and embedding the different parts together. Note that the strengthened numerical model was only hit in this section by El-Centro (1940) earthquake.

The results, detailed in Figure 9, indicate that adopting this strengthening solution decreases the amount of silos' displacement provoked by the seismic load significantly. In fact, the displacement at top of the silos decreases on average from 62 cm (fixed-based case) to 31 cm (SSI case) and 12 cm (SSI-reinforced case). SSI case refers to the reinforced numerical model while SSI case refers to the tilted silos, rested on the original/unstrengthen pile cap embedded

in the soil domain. For example, the displacement at top of silo#89, increases from 19.93 cm (static condition, displacement in February 2023) to 68 cm and 33.57 cm for the fixed-based and SSI cases while it decreases to 10 cm for the SSI-reinforced case.

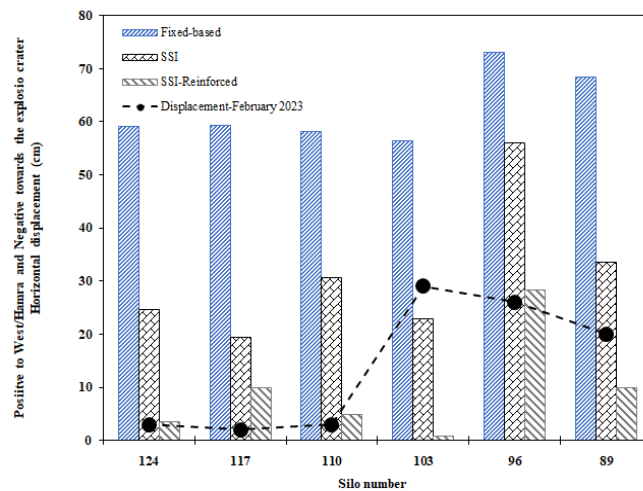


Figure 9: Maximum horizontal displacements at top of the South silos under El-Centro (1940).

6 CONCLUSIONS

Beirut port silos' structural health response was monitored since August 4, 2020 using 3D laser scan measurements and triaxial inclinometers installed on strategic locations on the South and North block silos. Since Lebanon is in an active seismic zone, the behavior of the remaining standing South block silos was simulated in this paper using the Finite Element Software Abaqus following different seismic loadings. Moreover, following the decision of the Lebanese authorities to preserve the remaining tilted standing silos to serve as a memorial for August 4, 2020 explosion, a repair and strengthening method of the South block silos is presented. The obtained results showed that:

- The remaining standing South block silos will be highly tilted under any earthquake loading. The horizontal displacements of the stable South block silos increase from 3 to 30 cm (static condition, in February 2023) up to 73 cm under El-Centro (1940), while they decrease up to -1 cm under Loma Prieta (1989) and Alkion (1981), respectively. Moreover, only 30% of the silos' surface undergoes some level of damage.
- Any seismic load experienced in Lebanon will cause an important tilting in the remaining standing silos ending in severe damage and high-risk of collapse.
- The strengthened solution consisting of increasing the silos' wall thickness from 29 to 41 cm, extending the pile cap an additional 3 X 1.12 m from the sides and inserting 15 m length 30 X 30 cm square driven piles every 1 m below the new pile cap improves the behavior of the remaining standing silos under seismic conditions.

ACKNOWLEDGMENT

The authors would like to acknowledge Eng. Emmanuel Durand (Amann Engineering), M. Christoph Fröhlich, Chris Held from Zoller and Fröhlich GmbH ("Z+F") for their logistics and financial efforts for using the Z+F Imager 5010X scanner (Zoller & Fröhlich) and Move Solutions for using and installing the triaxial inclinometers.

REFERENCES

- [1] S.W. Doebling, C.R. Farrar, M.B. Prime, D.W. Shevitz. *Damage identification and health monitoring of structural and mechanical systems from changes in their vibration characteristics: a literature review*. Los Alamos National Laboratory report LA13070-MS, 1996.
- [2] H. Sohn, C.R. Farrar, F.M. Hemez, D.D. Shunk, D.W. Stinemates, B.R. Nadler. *A review of structural health monitoring literature: 1996–2001*. Report LA-13976-MS. Los Alamos National Laboratory, 2004.
- [3] S. Das, P. Saha, S.K. Patro, Vibration-based damage detection techniques used for health monitoring of structures: a review. *Journal of Civil Structural Health Monitoring*, **6**, 447–507. 2016. doi: 10.1007/s13349-016-0168-5.
- [4] J. P. Lynch, K.J. Loh, A summary review of wireless sensors and sensor networks for structural health monitoring. *Shock Vibration Digest*, **38**, 91–130, 2006. doi: 10.1177/0583102406061499
- [5] C.B. Yun, J. Min, Smart sensing, monitoring, and damage detection for civil infrastructures. *KSCE Journal of Civil Engineering*, **15**, 1–14, 2011. doi: 10.1007/s12205-011-0001-y.
- [6] Y. Yu, W.H. Kang, C. Zhang, J. Wang, J. Ou, A stochastic analysis framework for a steel frame structure using wireless sensor system measurements. *Measurement*, **69**, 202–209, 2015. doi: 10.1016/j.measurement.2015.03.022.
- [7] H.T. Al-Khateeb, H.W. Shenton, M.J. Chajes, C. Aloupis, Structural Health Monitoring of a Cable-Stayed Bridge Using Regularly Conducted Diagnostic Load Tests, *Frontiers in Built Environment*, **5**, 41, 2019. doi: 10.3389/fbuil.2019.00041.
- [8] K. Aono, H. Hasni, O. Pochettino, N. Lajnef, S. Chakrabartty, Quasi-Self-Powered Piezo-Floating-Gate Sensing Technology for Continuous Monitoring of Large-Scale Bridges. *Frontiers in Built Environment*, **5**, 29, 2019. doi: 10.3389/fbuil.2019.00029.
- [9] How powerful was the Beirut blast Reuters Graphics, <https://graphics.reuters.com/LEBANONSECURITY/BLAST/yzdpxnmqbpv/>, 2020.
- [10] S. Rigby, T. Lodge, S. Alotaibi, A. Barr, S. Clarke, G. Langdon, A. Tyas, Preliminary yield estimation of the 2020 Beirut explosion using video footage from social media, *Shock Waves*, 2020. <https://doi.org/10.1007/s00193-020-00970-z>.
- [11] J. Diaz, Explosion analysis from images: Trinity and Beirut, *arXiv preprint arXiv:2009.05674*, 2020.
- [12] S. Ismail, W. Raphael, E. Durand, F. Kaddah, F. Geara, Analysis of the structural response of Beirut port concrete silos under blast loading, *Archives of Civil Engineering*, **67:3**, 619-638, 2021. doi: 10.24425/ace.2021.138074.
- [13] S. Ismail, W. Raphael, E. Durand, Monitoring the Beirut port silos structural health response few months after blast loading, *Jordan Journal of Civil Engineering*, **15:3**, 489-505, 2021.
- [14] S. Ismail, W. Raphael, E. Durand, Case study of the Beirut port explosion using 3D laser scan and nonlinear finite element model, *Research on Engineering Structures and Materials*, **7:4**, 551-577. doi: 10.17515/resm2021.286st0428.

- [15] S. Ismail, W. Raphael, E. Durand, F. Kaddah, Soil structure interaction effect on blast numerical analysis of Beirut port silos, *The Mediterranean Geosciences Union (MedGU2021)*, Istanbul, Turkey, 2021.
- [16] C. Stennett, S. Gaultier, J. Akhavan, An estimate of the TNT-equivalent net explosive quantity (NEQ) of the Beirut port explosion using publicly available tools and data, *Journal of Propellants, Explosives and Pyrotechnics*, **45**, 1675-1679, 2020, doi: 10.1002/ prep.202000227.
- [17] H. Pasman, C. Fouchier, S. Park, N. Quddus, D. Laboureur, Beirut ammonium nitrate explosion: Are we really not learning anything, *Journal of Process Safety*, **39**, e12203. 2020. doi:10.1002/ prs.12203.
- [18] G. Valsamos, M. Larcher, F. Casadei, Beirut explosion 2020: A case study for a large-scale urban blast simulation, *Journal of Safety Science*, **137**, 105190, 2021. doi: 10.1016/j.ssci.2021.105190.
- [19] K. Kawashima, Y. Takahashi, H. Ge, Z. Wu, J. Zhang, Reconnaissance report on damage of bridges in 2008 Wenchuan, China, earthquake, *Journal of Earthquake Engineering*, **13**, 956–998, 2009. doi:[10.1080/13632460902859169](https://doi.org/10.1080/13632460902859169).
- [20] H. Daou, W. Abou Salha, W. Raphael, A. Chateauneuf, Explanation of the collapse of Terminal 2E at Roissy–CDG Airport by nonlinear deterministic and reliability analyses, *Case Studies in Construction Materials*, **10** , 2214-5095, 2019. [doi: 10.1016/j.cscm.2019.e00222](https://doi.org/10.1016/j.cscm.2019.e00222).
- [21] Z. Chen, X. Li, Y. Yang, S. Zhao, Z. Fu, Experimental and numerical investigation of the effect of temperature patterns on behaviour of large scale silo, *Engineering Failure Analysis*, **91**, 543–53, 2018. doi: 10.1016/j.engfailanal.2018.04.043.
- [22] A. Y. Elghazouli, J. M. Rotter, Long-term performance and assessment of circular reinforced concrete silos, *Construction Building Material*, **10(2)**, 117–22, 1996. doi:10.1016/0950-0618(95)00091-7.
- [23] F. Giuliani, A. De Falco, S. Landi, M. Giorgio Bevilacqua, L. Santini, S. Pecori, Reusing grain silos from the 1930s in Italy. A multi-criteria decision analysis for the case of Arezzo, *Journal of Culture Heritage*, **29**, 145–59, 2018. doi:10.1016/j.culher.2017.07.009.
- [24] AFP, 2020 <https://english.alarabiya.net/features/2020/08/11/Beirut-explosion-Six-sources-explain-details-shine-light-on-Hezbollah-link>.
- [25] S. Sumitro, H. Matsuda, S. Nishimura, Application of smart 3-D laser scanner in structural health monitoring, *Computer Science*, 9693818, 2007. doi: 10.1201/9781439828441.ch290.
- [26] K. Kerhart, Spšp pardubice: Construction of a grain silo in Beirut, *Czech Civil Engineering Journal*, **3**, 1971.
- [27] C. Huijer, M. Harajli, S. Sadek, Upgrading the seismic hazard of Lebanon in light of the recent discovery of the offshore thrust fault system, *Lebanese Science Journal*, **12**, 2, 2011.
- [28] S. Ismail, F. Kaddah, W. Raphael, Seismic soil structure interaction response of midrise concrete structures on silty sandy soil, *Jordan Journal of Civil Engineering*, **14**, 1, 117-135, 2020.